Bifurcation analysis of double-diffusive convection with opposing horizontal thermal and solutal gradients

Shihe Xin,[a] Patrick Le Quéré,[b] and Laurette S. Tuckerman
LIMSI-CNRS, BP 133, 91403 Orsay Cedex, France

(Received 1 July 1997; accepted 29 December 1997)

The onset of convection in double diffusion with equal and opposite thermal and solutal buoyancy forces is studied. Numerical linear stability analyses and integration of the full Boussinesq equations are performed in an infinite vertical fluid layer and in closed rectangular cavities bounded by rigid walls. Detailed study of the subsequent nonlinear evolution is carried out for $Le=1.2$ and $Pr=1$. In the infinite vertical layer, the onset of convection is found to correspond to a subcritical circle pitchfork bifurcation. The finite-amplitude branch of steady states in turn loses stability to traveling waves via a supercritical drift pitchfork bifurcation. In a square cavity the bifurcation is transcritical and the full branch of stable and unstable solutions is constructed. With increasing cavity aspect-ratio, we observe alternating transcritical and pitchfork bifurcations, depending on the symmetry of the most unstable eigenvector. © *1998 American Institute of Physics.* [S1070-6631(98)02804-9]

I. INTRODUCTION

In laboratories and in the natural world, many convective phenomena involve both heat and mass transfer. Many configurations involving both vertical and horizontal temperature and concentration gradients have revealed intriguing instability phenomena;[1–13] see also Ref. 14 for a review. We investigate an infinite vertical fluid layer or finite cavity subjected to horizontal temperature and concentration gradients; these can be considered prototype configurations relevant in materials processing. We furthermore restrict our attention to thermal and solutal buoyancy forces which are of opposite sign and equal in magnitude. In this case there exists a trivial solution with zero velocity and linear temperature and concentration profiles, with isotherms and isoconcentration lines parallel to the vertical walls. When the Rayleigh number is increased, the conductive solution loses stability and convection is observed. After the original numerical and experimental study by Thorpe, Hutt, and Soulsby,[1] this case was studied numerically by Krishnan,[2] by Gobin and Bennacer,[3,4] and by Ghorayeb and Mojtabi.[5,6]

Thorpe *et al.*[1] and Gobin and Bennacer[3,4] calculated the linear stability of a vertically infinite fluid layer between free-slip sidewalls. They assumed that the eigenvalue was real and that the eigenmode consisted of inclined cells whose angle of inclination and wavelength was chosen to minimize the critical Rayleigh number. These assumptions were justified *a posteriori* by subsequent more general analyses[5–7] which calculated a slightly higher threshold for rigid sidewalls. However, the nonlinear behavior after the onset of convection has until now remained unexplored. We have conducted numerical integration of the full Boussinesq equations in a vertical slot and discovered unexpected new behavior, in particular, finite-amplitude traveling waves. We have undertaken the present study to elucidate the nature of the corresponding bifurcations.

Gobin and Bennacer also carried out numerical simulations in a square cavity with rigid walls. They found that convection appeared at Rayleigh numbers close to those calculated for the infinite fluid layer. The agreement between critical Rayleigh numbers for the square cavity and the infinite fluid layer might at first appear to mutually validate both results. However, the rigid walls of the square cavity strongly confine the flow, and one would generally expect the threshold in the square cavity to be much higher than that in the infinite layer. This stabilizing effect should be especially marked, given that the eigenmode in the infinite layer is strongly inclined and thus not well accommodated in a square cavity. Indeed, this suspicion was borne out by the discovery[5–7] that the bifurcation to convection in a square cavity was transcritical: What had been observed in Refs. 3 and 4 was not the linear threshold but the saddle-node bifurcation terminating a finite-amplitude branch. Here we have used new numerical techniques to construct the full solution branch of stable and unstable steady states by adapting a time-dependent code to carry out Newton's method and continuation. We have also calculated the thresholds for transcritical and pitchfork bifurcations for aspect ratios up to $A=4$.

In Sec. II, we present the governing equations in the two geometries investigated, along with their symmetries, and the numerical methods used. Numerical results are discussed in Sec. III and concluding remarks are given in Sec. IV.

II. DESCRIPTION OF THE PROBLEM AND METHODS

A. Governing equations

Consider a binary fluid confined between two vertical rigid walls separated by a distance L, each of which is maintained at a fixed temperature and concentration. We consider

[a]Current address: Dept. of Mech. Engineering, University of Surrey, Guildford GU2 5XH, UK.
[b]Corresponding author. Electronic mail: plq@limsi.fr

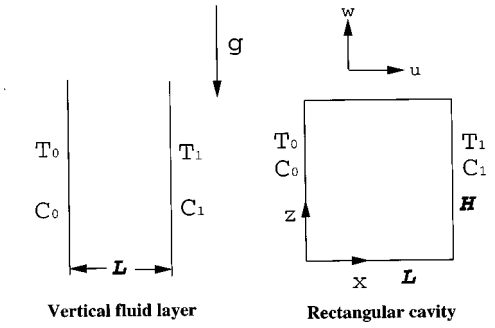

FIG. 1. Cavity configurations.

both an infinite vertical slot and a rectangular cavity with rigid adiabatic horizontal walls, as depicted in Fig. 1. The temperature and concentration differences imposed between the vertical walls are $\Delta T = T_0 - T_1$ and $\Delta C = C_0 - C_1$. The binary fluid's properties are given by its kinematic viscosity ν, its thermal and solutal diffusivities κ and D, and its thermal and solutal expansion coefficients β_T and β_C. We assume that the Dufour and Soret effects can be neglected and that the Boussinesq approximation holds: In the buoyancy term, the fluid density is thus expanded as $\rho(T,C) = \rho_0(T_r,C_r)[1-\beta_T(T-T_r)-\beta_C(C-C_r)]$ where $T_r = (T_0 + T_1)/2$ and $C_r = (C_0 + C_1)/2$.

The equations are nondimensionalized by defining the reduced temperature $\Theta \equiv (T-T_r)/(T_0-T_1)$ and the reduced concentration $\mathscr{C} \equiv (C-C_r)/(C_0-C_1)$ and by scaling length by the distance L between the vertical walls and time by $L^2/(\kappa\sqrt{Ra})$, where Ra is the thermal Rayleigh number $Ra = (g\beta_T \Delta T L^3)/(\nu\kappa)$. The dimensionless Boussinesq equations then read

$$\frac{\partial U}{\partial x} + \frac{\partial W}{\partial z} = 0, \tag{1a}$$

$$\frac{\partial U}{\partial t} + U\frac{\partial U}{\partial x} + W\frac{\partial U}{\partial z} = -\frac{\partial P}{\partial x} + \frac{Pr}{\sqrt{Ra}}\nabla^2 U, \tag{1b}$$

$$\frac{\partial W}{\partial t} + U\frac{\partial W}{\partial x} + W\frac{\partial W}{\partial z} = -\frac{\partial P}{\partial z} + \frac{Pr}{\sqrt{Ra}}\nabla^2 W + Pr\left(\Theta + \frac{1}{Le}\frac{Ra_C}{Ra}\mathscr{C}\right), \tag{1c}$$

$$\frac{\partial \Theta}{\partial t} + U\frac{\partial \Theta}{\partial x} + W\frac{\partial \Theta}{\partial z} = \frac{1}{\sqrt{Ra}}\nabla^2 \Theta, \tag{1d}$$

$$\frac{\partial \mathscr{C}}{\partial t} + U\frac{\partial \mathscr{C}}{\partial x} + W\frac{\partial \mathscr{C}}{\partial z} = \frac{1}{Le\sqrt{Ra}}\nabla^2 \mathscr{C}, \tag{1e}$$

where U,W are dimensionless velocity components, $Ra_C \equiv (g\beta_C \Delta C L^3)/(\nu D)$ is the solutal Rayleigh number, Pr is the Prandtl number ν/κ and Le is the Lewis number κ/D.

The flow domain is $(x,z) \in [0,1]\times[0,A]$ for the finite cavity where $A = H/L$ is the cavity aspect ratio. The vertically infinite fluid layer is assumed periodic, i.e, $(x,z) \in [0,1]\times[0,\lambda]$ where λ is the imposed wavelength. The vertical walls are rigid and conducting, while the horizontal walls of the finite cavity are rigid and adiabatic. The boundary conditions are

$$U = W = \Theta - 0.5 = \mathscr{C} - 0.5 = 0 \quad \text{at } x = 0, \tag{2a}$$

$$U = W = \Theta + 0.5 = \mathscr{C} + 0.5 = 0 \quad \text{at } x = 1, \tag{2b}$$

$$U, W, \Theta, \mathscr{C} \quad \lambda\text{-periodic in } z \text{ (infinite cavity)}, \tag{2c}$$

$$U = W = \frac{\partial \Theta}{\partial z} = \frac{\partial \mathscr{C}}{\partial z} = 0 \quad \text{at } z = 0, A \text{ (rectangular cavity)}. \tag{2d}$$

We will consider only the case in which the buoyancy forces due to the thermal and solutal gradients are equal and opposite, i.e., we set the buoyancy number to -1

$$N \equiv \frac{Ra_C}{LeRa} = \frac{\beta_T \Delta T}{\beta_C \Delta C} = -1. \tag{3}$$

In the remainder of the article, we will thus fix $Ra_C = -LeRa$ and dispense with the parameter Ra_C. In this case, Eqs. (1) with boundary conditions (2) possess the trivial conductive solution $\overline{U} = \overline{W} = 0$ and $\overline{\Theta}(x,z) = \overline{\mathscr{C}}(x,z) = 0.5 - x$. In order to study the stability of the conductive solution, let us write Eqs. (1) in perturbation form. Using $u = U - \overline{U}$, $w = W - \overline{W}$, $\theta = \Theta - \overline{\Theta}$, and $c = \mathscr{C} - \overline{\mathscr{C}}$, Eq. (1) become

$$\frac{\partial u}{\partial x} + \frac{\partial w}{\partial z} = 0, \tag{4a}$$

$$\frac{\partial u}{\partial t} + u\frac{\partial u}{\partial x} + w\frac{\partial u}{\partial z} = -\frac{\partial P}{\partial x} + \frac{Pr}{\sqrt{Ra}}\nabla^2 u, \tag{4b}$$

$$\frac{\partial w}{\partial t} + u\frac{\partial w}{\partial x} + w\frac{\partial w}{\partial z} = -\frac{\partial P}{\partial z} + \frac{Pr}{\sqrt{Ra}}\nabla^2 w + Pr(\theta - c), \tag{4c}$$

$$\frac{\partial \theta}{\partial t} - u + u\frac{\partial \theta}{\partial x} + w\frac{\partial \theta}{\partial z} = \frac{1}{\sqrt{Ra}}\nabla^2 \theta, \tag{4d}$$

$$\frac{\partial c}{\partial t} - u + u\frac{\partial c}{\partial x} + w\frac{\partial c}{\partial z} = \frac{1}{Le\sqrt{Ra}}\nabla^2 c. \tag{4e}$$

The corresponding boundary conditions are homogeneous

$$u = w = \theta = c = 0 \quad \text{at } x = 0,1, \tag{5a}$$

$$u, w, \theta, c \quad \lambda\text{-periodic in } z \text{ (infinite cavity)}, \tag{5b}$$

$$u = w = \frac{\partial \theta}{\partial z} = \frac{\partial c}{\partial z} = 0 \quad \text{at } z = 0, A \text{ (rectangular cavity)}. \tag{5c}$$

The linearized evolution equations are obtained by setting the nonlinear terms in Eqs. (4) to zero. When $Le = 1$, the conductive solution is stable for all Rayleigh numbers, for the following reason: Because the diffusion times of θ and c are equal, the linearized versions of Eqs. (4d)–(4e) imply that $(\theta - c)$ obeys a diffusion equation. With homogeneous boundary conditions, $(\theta - c)$ always decays to zero, and so the buoyancy force $Pr(\theta - c)$ of Eq. (4c) cannot be maintained. When $Le \neq 1$, the diffusion times for temperature and

concentration are no longer equal and this argument no longer holds. We denote by Ra_c the critical thermal Rayleigh number above which the conductive solution is unstable. It can easily be shown from Eqs. (4) that, for a steady bifurcation, $Ra_c(Le-1)$ is a constant that depends only on the boundary conditions and is independent of Prandtl number. One consequence is that Ra_c is infinite for $Le=1$, as argued above.

B. Numerical methods

Except for the linear stability analysis of the vertical slot, all of our calculations are based on two pseudospectral time-stepping codes,[15] which we have adapted to directly calculate eigenvectors and bifurcation points. The basis functions in x are Chebyshev polynomials. In z, we use Fourier series for the vertical slot and Chebyshev polynomials for the rectangular cavity. For the vertical slot, we use $N_x=30$ modes in x, with a single Fourier mode for the linear stability analysis, and with $N_z=32$ modes for nonlinear calculations. For rectangular cavities, we use $N_x=40$ Chebyshev polynomials or gridpoints, and N_z ranging from $N_z=40$ for the square cavity $A=1$ to $N_z=120$ for $A=4$. Our time-stepping scheme is second order and combines numerical differentiation (e.g., Ref. 16) for the linear terms with Adams–Bashforth for the nonlinear terms. Incompressibility is enforced by a direct Uzawa method.[17] More details concerning the method can be found in Ref. 18.

For the linear stability analysis of the vertical slot, the eigenmodes are of the form $(\psi,\theta,c)(x,z,t)=(\hat{\psi},\hat{\theta},\hat{c})(x)\times\exp[i\alpha z+\sigma t]$, where ψ is the streamfunction. The eigenvalue problem for $(\hat{\psi},\hat{\theta},\hat{c})(x)$ resulting from linearizing Eqs. (4) with boundary conditions (5a) is discretized by Chebyshev collocation[15] and is solved with subroutines from the NAG software library; see Ref. 19 for more details. For each α, the value of Ra at which $Re(\sigma)=0$ is found and the neutral curve is then constructed.

In a rectangular cavity with rigid walls, the eigenmodes are no longer trigonometric in z, and so their dependence on z as well as on x must be determined numerically. Our discrete operators are of size $4\times N_x\times N_z$, i.e., between 6400 and 19 200 for our study. We therefore use a version of the iterative power method to find only the eigenvalues of interest: By integrating the linearized version of Eqs. (4) with boundary conditions (5a) and (5c) in time, we are effectively acting repeatedly with the exponential of the Jacobian $\exp(J)$, whose dominant eigenvalues (those of largest magnitude) are the leading eigenvalues (those of largest real part) of J. In order to find several leading eigenvalues, Arnoldi's method can be used. The details are described in Refs. 20–22. In order to calculate unstable solutions, we adapted the time-stepping code to carry out Newton's method for steady state solving, as described in Refs. 22–24. Far from turning points, an initial guess for each solution (u,w,θ,c) along the branch is obtained by quadratic extrapolation in Ra. This fails near a turning point, and one must consider instead that Ra and all but one selected field component $\tilde{w}$, here typically w $(x=0.75, z=0.25)$, are quadratic functions of $\tilde{w}$. We found that considering Ra as a dependent variable in the predictor phase—i.e., in choosing an initial guess—sufficed to allow us to go around turning points without having to consider Ra as a dependent variable in the corrector phase—i.e., in the Newton iteration.

We used Newton's method to calculate steady bifurcation points. The linearized version of Eqs. (4) with $\partial/\partial_t=0$ and boundary conditions (5a) and (5b) or (5a) and (5c) can be considered to be a nonlinear set of equations for the critical eigenvector and Rayleigh number. The eigenvector is normalized by fixing one of its components, and the Rayleigh number becomes one of the unknowns. Newton's method determines directly and precisely the critical Rayleigh number and corresponding eigenvector. The algorithm for adapting the time-stepping code to carry out this procedure is given in Ref. 24.

C. Symmetries

1. Rectangular cavities: Z_2

In a rectangular cavity, of aspect ratio A, Eqs. (4) with boundary conditions (5a) and (5c) are invariant under combined reflection by x and z (or, equivalently, under rotation by π) and by the inversion of the temperature and concentration perturbation fields. Formally this can be described by the action of the operator S defined by

$$S\begin{Bmatrix}\psi\\ \theta\\ c\end{Bmatrix}(x,z)\equiv\begin{Bmatrix}\psi\\ -\theta\\ -c\end{Bmatrix}(1-x,A-z), \tag{6}$$

where ψ is the streamfunction. If (ψ,θ,c) is a solution to Eqs. (4), (5a), and (5c), then so is $S(\psi,\theta,c)$, i.e., Eqs. (4), (5a), and (5c) possess centro-symmetry.

For the corresponding linearized problem, eigenmodes will be either centro-symmetric, i.e., $S(\psi,\theta,c)=(\psi,\theta,c)$, or anti-centro-symmetric, i.e., $S(\psi,\theta,c)=-(\psi,\theta,c)$. Centro-symmetric eigenmodes contain an odd number of cells while anti-centro-symmetric eigenmodes contain an even number of cells. If a critical eigenmode is centro-symmetric, then the corresponding bifurcation occurring in Eqs. (4), (5a), and (5c) is transcritical, while if a critical eigenmode is anti-centro-symmetric, then the corresponding bifurcation is a pitchfork. $\{I,S\}$ is the group Z_2, and the facts we have listed above constitute the theory of bifurcation under Z_2 symmetry. See, e.g., Crawford and Knobloch[25] for more details.

2. Vertical layer: $O(2)$

In a vertically periodic slot with period λ, problem (4), (5a), and (5b) retains centro-symmetry, with the replacement of $(A-z)$ in Eq. (6) by $(\lambda-z)$. The problem also possesses the additional symmetry of z-translation by any $\hat{z}$, described by the operator

$$R_{\hat{z}}\begin{Bmatrix}\psi\\ \theta\\ c\end{Bmatrix}(x,z)\equiv\begin{Bmatrix}\psi\\ \theta\\ c\end{Bmatrix}(x,z+\hat{z}\bmod\lambda). \tag{7}$$

Transformations (6) and (7) constitute a representation of the group $O(2)$; see, e.g., Ref. 25.

The eigenmodes which are solutions to the linearized problem are expected to break the translational symmetry. Hence, each eigenmode belongs to a ''circle'' of eigenmodes, related to one another by z-translation and sharing a common eigenvalue. For each eigenmode, there exists a z_0 about which it is centro-symmetric, i.e.

$$(\psi,\theta,c)(x,z)=(\psi,-\theta,-c)(1-x,(\lambda-z+z_0)\text{mod }\lambda),$$

whereas it is anti-centro-symmetric about $(z_0+\lambda/4)$ mod λ. The bifurcations of Eqs. (4), (5a), and (5b) from conduction to convection lead to circles of equivalent steady states related to each other by z-translation, and are called circle pitchforks. These nonlinear steady states are, like the eigenmodes, centro-symmetric about some z_0, but they are not anti-centro-symmetric about $(z_0+\lambda/4)$ mod λ.

The steady states are susceptible to a further bifurcation, called a drift pitchfork,[26–30] which breaks the centro-symmetry and leads to traveling waves whose wavespeed at onset vanishes. The eigenvalue associated with a drift pitchfork is zero at the bifurcation. This should be compared with a Hopf bifurcation, which is associated with a pair of complex conjugate eigenvalues and leads to traveling waves whose wave speed is finite at onset.

This sequence of bifurcations, or scenario, is often described by the following set of ordinary differential equations, or normal form:

$$\dot{a}=(\mu-a^2)a, \tag{8a}$$

$$\dot{z}=s, \tag{8b}$$

$$\dot{s}=(a^2-1-s^2)s. \tag{8c}$$

The reflection and rotation symmetry operators S and $R_{\hat{z}}$ for the normal form are

$$S(a,z,s)\equiv(a,\lambda-z,-s), \tag{9a}$$

$$R_{\hat{z}}(a,z,s)\equiv(a,z+\hat{z}\text{ mod }\lambda,s). \tag{9b}$$

Equations (8) have $O(2)$ symmetry, an essential requirement for the circle and drift pitchfork scenario, meaning that if (a,z,s) is a solution, then so are $S(a,z,s)$ and $R_{\hat{z}}(a,z,s)$.

In Eqs. (8), μ is a bifurcation parameter, analogous to $Ra-Ra_c$. The variable a represents the amplitude of convection. The λ-periodic variable z can be thought of as the location of some distinguished feature of the flow, e.g., a velocity maximum, vortex center, or stagnation point. The variable s represents a possible translational velocity. The conductive state corresponds to $a=s=0$. Equation (8a) undergoes a pitchfork bifurcation at $\mu=0$, leading to steady states $a=\sqrt{\mu}$ of arbitrary phase $z=z_0$, and zero velocity $s=0$. This is a circle pitchfork bifurcation for the system (8). Equation (8c) then undergoes a pitchfork bifurcation at $\mu=1$, leading to time-dependent solutions $a=\sqrt{\mu}$ with ''drifting'' phase $z=z_0+st$, whose velocity $s=\pm\sqrt{\mu-1}$ is proportional to the square root of the distance from threshold. Two circles of traveling wave solutions are created: Both upwards-moving $(s=\sqrt{\mu-1})$ and downwards-moving $(s=-\sqrt{\mu-1})$ solutions exist and are dynamically equivalent, and the solutions are also characterized by their initial phase z_0. This is a drift pitchfork bifurcation for system (8a)–(8c).

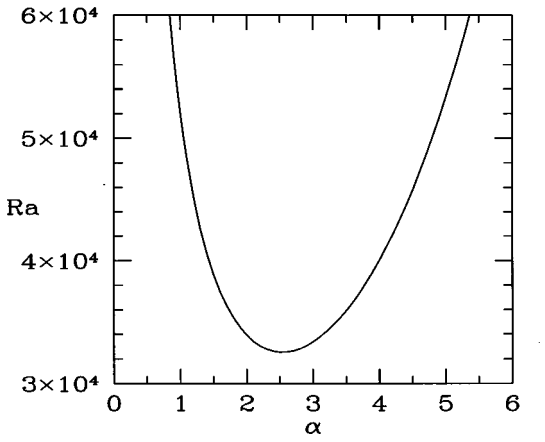

FIG. 2. Neutral curve for $Le=1.2$ in a vertical fluid layer. $Ra_c=32\,545\pm10$ and $\alpha_c=2.52\pm0.01$.

One or both of the pitchfork bifurcations may be made subcritical, by changing the sign of the a^2 term in Eq. (8a) or of the s^2 term in Eq. (8c) and adding higher order terms.

We will see examples of circle and drift pitchfork bifurcations in the next section.

III. RESULTS

A. Vertical layer

We have investigated several Prandtl numbers and Lewis numbers. We find $Ra_c(Le-1)=6509\pm2$, in agreement with Ghorayeb and Mojtabi.[5,6] The lower values 6137 and 6122 reported by Thorpe *et al.*[1] and by Gobin and Bennacer,[3,4] respectively, are easily attributed to the boundary conditions: The sidewalls of our configuration are rigid, while those in Refs. 1, 3, and 4 are free-slip. For $Le=1.2$ the neutral curve is displayed in Fig. 2. The minimum is at $Ra_c=32\,545$, $\alpha_c=2.52$, in agreement with Ghorayeb and Mojtabi's value of 2.53. The critical wave number α_c is independent of both Prandtl and Lewis numbers. The critical wavelength is $\lambda_c=2\pi/\alpha_c=2.50$.

The corresponding critical eigenfunction, shown in Fig. 3, consists of inclined cells similar to those depicted origi-

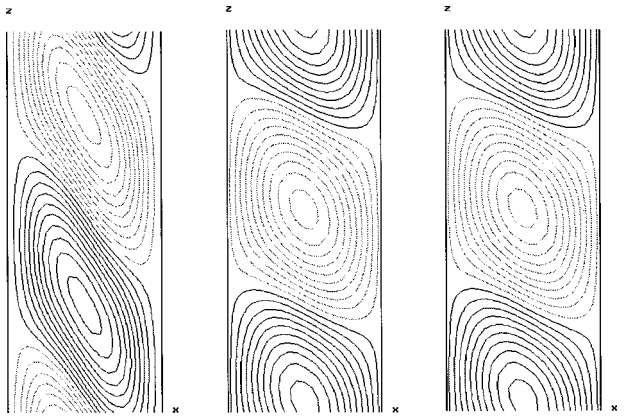

FIG. 3. Critical eigenvector in a vertical fluid layer at $Le=1.2$, $Ra_c=32\,545$, and $\alpha_c=2.52$. Left: Stream function. Middle: Temperature. Right: Concentration. Solid (dashed) contours denote positive (negative) values or circulation.

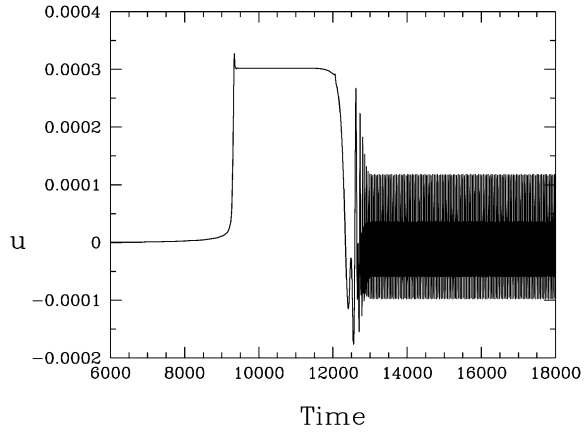

FIG. 4. Evolution in time of $-u(x=0.0423,z=0.8594)$ at $Ra=3.4\times10^4$ in a vertical fluid layer. The initial conductive state ($0<t<8500$) is succeeded by a plateau at an unstable finite amplitude state ($9500<t<11500$), and finally by stable oscillations ($t>13\,000$).

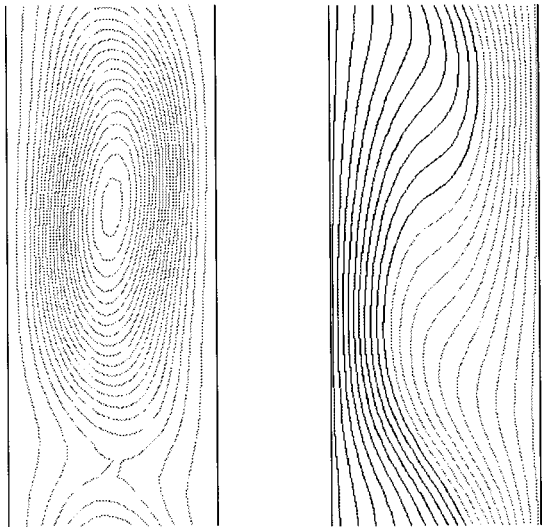

FIG. 5. Unstable finite amplitude solution at $Ra=3.4\times10^4$ in a vertical fluid layer. Left: Streamfunction. Right: Concentration.

nally by Thorpe *et al.*[1] We can understand the qualitative form of the eigenfunction physically by the following argument. Consider a fluid particle displaced rightwards towards increasing x, i.e., from a warmer and heavier environment to a cooler and lighter one. Initially, the particle is warmer and heavier than the fluid surrounding it; the former property would cause the particle to rise and the latter to fall. However, for $Le>1$, the particle's temperature equilibrates more rapidly to its environment than does its concentration. Heavier than the fluid surrounding it, the particle falls. Similarly, a fluid particle moved leftwards towards decreasing x will find itself lighter than its environment and thus will rise. This explains the direction in which the streamfunction contours are inclined: Contours are directed downwards and towards the colder wall if $Le>1$ and downwards and towards the denser wall if $Le<1$.

We also carried out numerical integration of Eqs. (4), (5a), and (5b) in a periodic computational domain of length $0\leqslant z<\lambda_c$. Figure 4 shows the time history of the numerical integration performed for $Ra=3.4\times10^4$, $Pr=1$, and $Le=1.2$. The initial part of the time series shows that the stationary conductive solution is unstable. During $8500<t<10\,000$, a transition occurs to the finite-amplitude steady state depicted in Fig. 5. This steady state is also seen to be unstable, and, after another rapid transition during $11\,500<t<13\,000$, is succeeded by the stable periodic solution depicted in Fig. 6.

We now discuss these two transitions in more detail. The eigenmode shown in Fig. 3 has broken the translational symmetry in z, but there exists a z_0 about which it is centro-symmetric. As discussed in Sec. II C, the bifurcation that occurs at Ra_c is a circle pitchfork, leading to a set of dynamically equivalent steady states parametrized by their phase in z. In order to determine whether the circle pitchfork bifurcation is supercritical or subcritical, we examine the temporal evolution in more detail. The logscale enlargement for $5000\leqslant t\leqslant11\,000$ shown in Fig. 7 shows that the linear amplification phase extends to $t\approx8500$ and that, subsequently, when nonlinear effects come into play, the slope increases. The u velocity shown in Figs. 4 and 7 can be thought of as representing the amplitude a of the bifurcating mode in a normal-form model like Eqs. (8). The fact that its slope increases after the linear phase of the evolution shows that the coefficient of the cubic term in the normal form is positive, thus proving that the pitchfork bifurcation is subcritical.[31] We have calculated the steady finite amplitude branch for decreasing values of Rayleigh number and located its turning point (saddle-node) at $Ra_s=24\,500$, considerably below $Ra_c=32\,545$, the value at which the conductive branch loses stability. We have also investigated other Prandtl and Lewis numbers, and the pitchfork bifurcation is subcritical in all of the cases we considered.

The finite-amplitude steady state which results from the circle pitchfork bifurcation is shown in Fig. 5. It differs markedly from the eigenmode shown in Fig. 3. One reason for this is the inclusion of the conductive solution in the concentration field shown in Fig. 5. However, the velocity fields of the eigenmode and of the finite-amplitude steady state are also quite different. The eigenmode consists of alternating clockwise and counter-clockwise vortices, separated by nearly straight boundaries. In contrast, the circulation in the finite-amplitude state is overwhelmingly negative; the flow consists of clockwise vortices separated by stagnation points. The critical eigenmode and finite-amplitude state resulting from a subcritical bifurcation are typically quite different: The finite-amplitude state is not well approximated as a superposition of the conductive state and the eigenmode. Finally, the finite-amplitude state is, like the eigenmode, centro-symmetric about some z_0, as discussed in Sec. II C. This is most clearly seen by examining streamlines near the stagnation point and vortex center.

Returning to the time series of Fig. 4, we now focus on the transition for $t>11\,500$ which leads to the traveling-wave state depicted in Fig. 6. By integrating Eqs. (4), (5a) and (5b) for several Rayleigh numbers, we found that the steady finite-amplitude states, such as that depicted in Fig. 5, are stable only for a very small range of Rayleigh number.

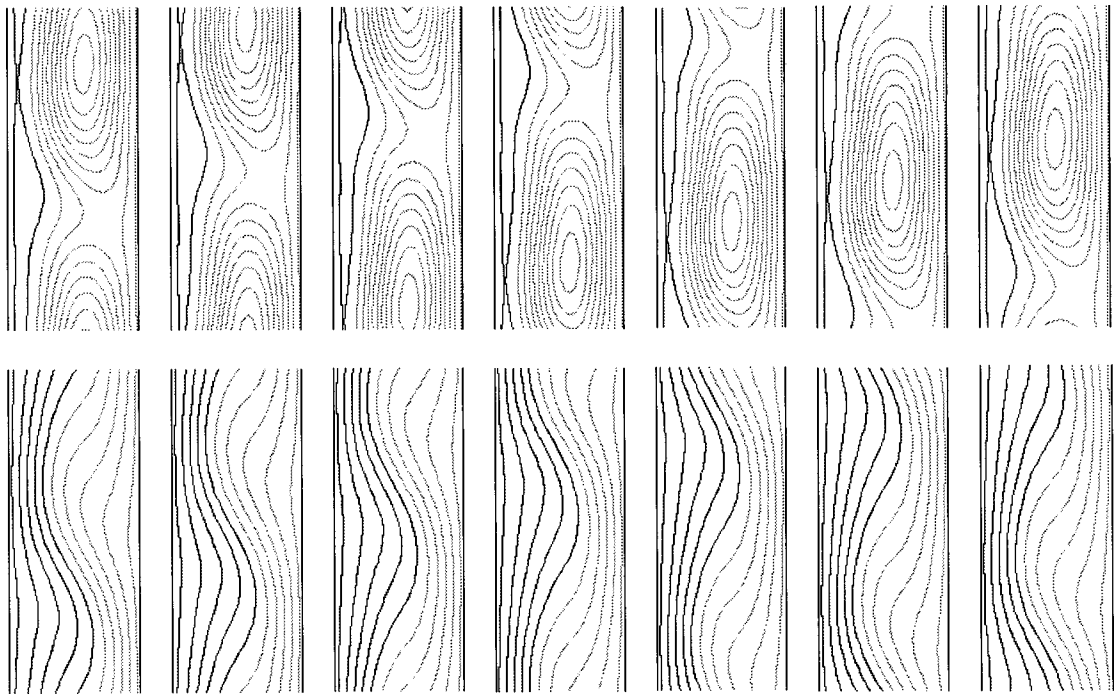

FIG. 6. Traveling waves at $Ra=3.4\times10^4$ in a vertical fluid layer. Above: Stream function. Below: Concentration. Unlike the unstable steady state, the instantaneous flows of the traveling wave are not centro-symmetric.

Above this range, the solution begins to drift slowly up or down, as shown in Fig. 6. This transition is the drift pitchfork bifurcation discussed in Sec. II C. Examination of the instantaneous streamlines near the stagnation point and the position of the vortex center shows that the traveling wave state in Fig. 6 is not centro-symmetric. We have computed the nonlinear traveling wave states for several Rayleigh numbers. Figure 8 shows that the wave speed s is proportional to $\sqrt{Ra-Ra_d}$, with the critical Rayleigh number for the drift bifurcation $Ra_d=2.9\times10^4$ determined by extrapolation. This relation, discussed in Sec. II C, confirms that the bifurcation is a drift pitchfork, and also establishes that it is supercritical.

The transition to convection in this system is highly hysteretic. We have seen that the transition observed upon slowly increasing Ra past $Ra_c=3.25\times10^4$ is from conduction directly to traveling waves of finite amplitude and speed, as a consequence of the fact that the Rayleigh number at which the drift pitchfork occurs is below that of the circle pitchfork. Upon decreasing the Rayleigh number, the wave speed decreases, vanishing at $Ra_d=2.9\times10^4$ and leading to a steady convective state. Further decrease of Ra past $Ra_s=2.45\times10^4$ leads to a transition from finite amplitude convection to conduction.

We summarize our results for $Le=1.2$ and $Pr=1$ by the qualitative bifurcation diagram sketched in Fig. 9. We believe that this scenario also holds qualitatively for neighbor-

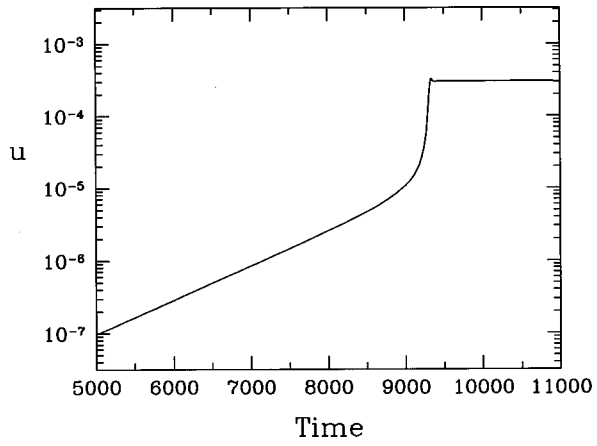

FIG. 7. Evolution of $\log[-u(x=0.0423,z=0.8594)]$ at $Ra=3.4\times10^4$ in a vertical fluid layer. Initial phase of exponential growth ($0<t<8500$) is followed by a *more rapid* nonlinear phase ($8500<t<9300$), indicating a subcritical bifurcation.

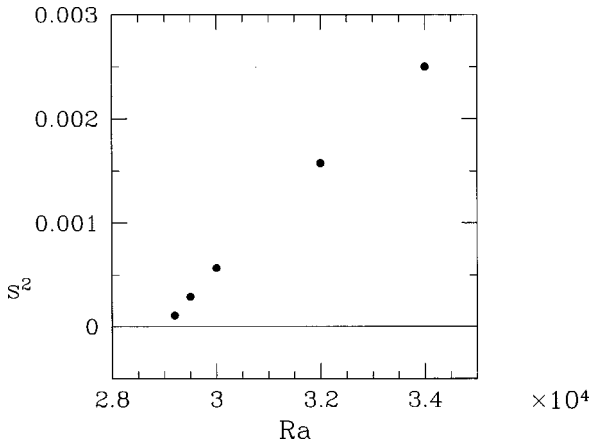

FIG. 8. Square of wave speed of traveling waves as a function of Ra in a vertical fluid layer. Straight line fit indicates a drift pitchfork at $Ra_d=2.9\times10^4$ determined by extrapolation.

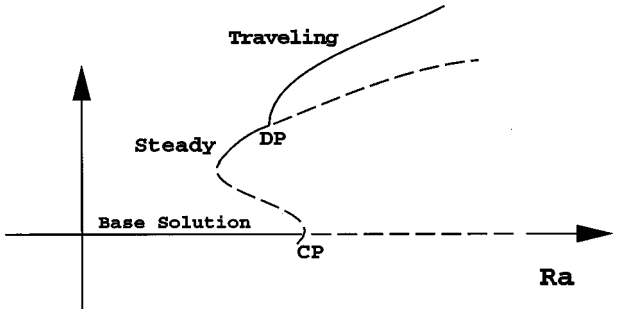

FIG. 9. Bifurcation diagram for $Le=1.2$ and $Pr=1$ in a vertical fluid layer. Circle pitchfork (CP) occurs at $Ra_c=32\,545$, drift pitchfork (DP) at $Ra_d=29\,000$, and the saddle node at $Ra_s=24\,500$.

ing values of Lewis and Prandtl numbers: The conductive branch becomes unstable via a subcritical circle pitchfork bifurcation and the resulting finite amplitude branch subsequently undergoes a drift pitchfork bifurcation.

B. Square and rectangular cavities

In a square cavity for $Le=1.2$, Gobin and Bennacer[3,4] located the onset of convection for Ra between 30 000 and 35 000 by carrying out direct numerical nonlinear simulations at these two Rayleigh numbers. However, linear stability analyses by Ghorayeb and Mojtabi[5,6] and by us[7] have shown that the conductive state is stable far beyond this, until $Ra_c=85\,820$. This discrepancy is due to the *transcriticality* of the bifurcation, combined with the fact that Gobin and Bennacer carried out sudden-start simulations from a uniform temperature rather than from the conductive solution (see, e.g., Fig. 9 of Ref. 4). The bifurcation diagram, computed via the continuation method described in Sec. II B, is displayed in Fig. 10, along with representative stable and unstable solutions from the upper and lower convective branches. We can term this bifurcation strongly transcritical: The saddle-node which we have localized at $Ra_s=29\,200$ is far from the transcritical bifurcation at $Ra_c=85\,820$, and the finite-amplitude states consisting of one large clockwise roll are very different from the three-roll small-amplitude states and eigenvector.

Although the first instability in the square cavity is via a transcritical bifurcation to a centro-symmetric eigenmode, as discussed in Sec. II C, we may also compute the threshold for a pitchfork bifurcation by seeking a critical eigenvector with anti-centro-symmetry. By imposing this symmetry, we find that the first pitchfork bifurcation in a square cavity occurs at $Ra_c=129491$ for $Le=1.2$. More generally, $Ra_c(Le-1)=25\,900$ for the first pitchfork bifurcation in a square cavity.

One can expect that increasing the cavity aspect ratio will cause the transcritical and pitchfork bifurcation thresholds, so widely separated in the square, to approach one another. We used continuation to follow the same eigenvector while increasing the cavity aspect ratio from 1 to 4. Critical Rayleigh numbers for the first transcritical and pitchfork bifurcations are shown in Fig. 11. Both thresholds decrease with increasing aspect ratio. The curves cross twice in this range; for $2.14\lesssim A\lesssim 3.4$ the first instability is a pitchfork bifurcation. This alternation of transcritical and pitchfork bifurcations with aspect ratio is typical of convection problems in finite cavities with rigid walls (e.g., Ref. 24). We present numerical values for the thresholds in terms of $Ra_c(Le-1)$ in Table I.

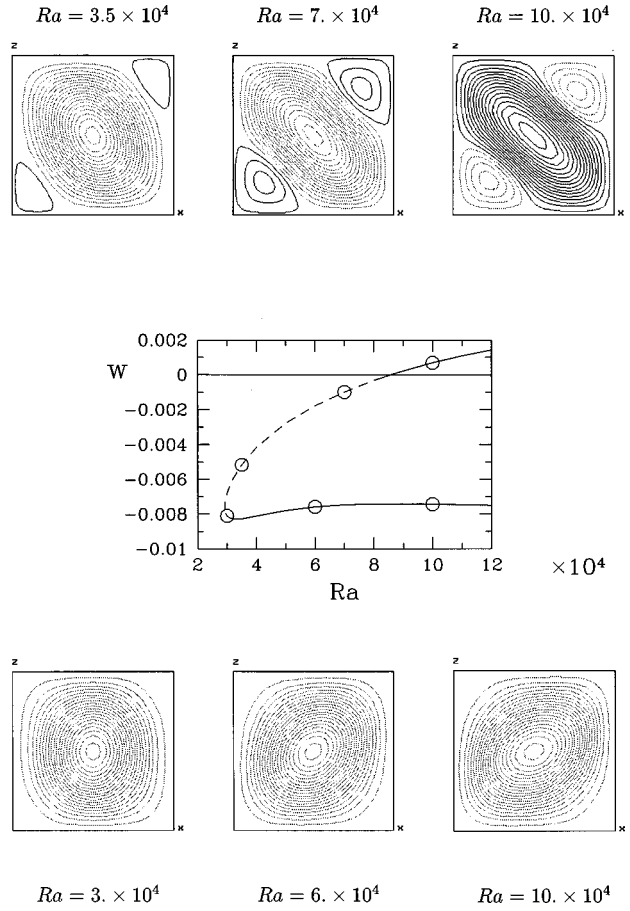

FIG. 10. Center: Bifurcation diagram for square cavity, $Le=1.2$. Transcritical bifurcation occurs at $Ra_c=85\,820$, saddle-node bifurcation at $Ra_s\approx 29\,200$. Solid and dashed portions of curve represent stable and unstable states, respectively. Above and below: Representative streamfunction contours along the upper and lower branches at designated values of Ra. Solid and dashed contours represent positive and negative circulation, respectively. Three-cell flow with large cell of positive (negative) circulation is stable (unstable). Flows on large-amplitude branch consist of one cell with negative circulation.

IV. DISCUSSION

We have investigated the onset of double diffusive convection in a vertical layer and in a closed cavity subjected to equal and opposite horizontal temperature and concentration gradients. Our philosophy has been to adapt time-stepping codes to perform all of the tasks needed for a full bifurcation analysis, i.e., linear stability analysis and continuation. The transition from conduction to convection in this system follows a variety of paths, depending on the geometry.

In a vertical slot, the initial instability of the conductive state is a subcritical circle pitchfork bifurcation leading to steady centro-symmetric convective states. The steady state is subsequently destabilized by a drift pitchfork bifurcation leading to traveling waves. The system shows hysteresis: In-

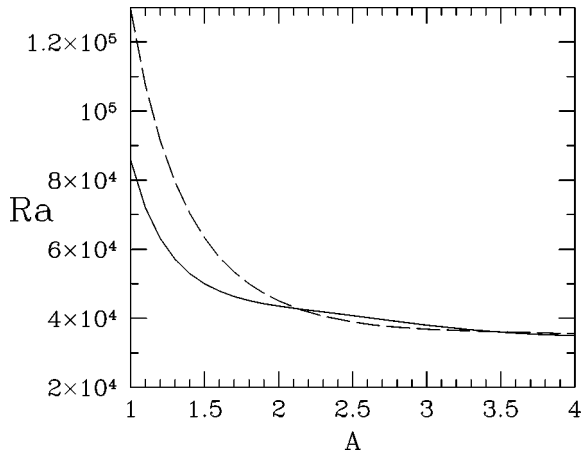

FIG. 11. Critical Rayleigh numbers for first transcritical (solid) and pitchfork (dashed) bifurcations for $Le=1.2$ as a function of aspect ratio. Curves cross at $A=2.14$ and at $A=3.45$.

creasing the Rayleigh number past the convective threshold leads directly to traveling waves of finite amplitude and wave speed, while decreasing the Rayleigh number leads first to steady finite-amplitude convection and subsequently to conduction. The finite-amplitude convective states—both steady and time-dependent—look quite different from the regular arrays of tilted vortices of the eigenmode.

In rectangular cavities of increasing height, we observe the classic alternation between critical Rayleigh numbers for transcritical and pitchfork bifurcations corresponding to centro-symmetric and anti-centro-symmetric eigenvectors, respectively. The distinction between the two types of eigenvectors disappears for the translationally invariant vertical slot, and the transcritical and pitchfork bifurcations are supplanted by a circle pitchfork.

While understanding the transitions undergone by the system in terms of bifurcations and symmetries is essential, a complementary physical or heuristic understanding would also be desirable. Analysis of the bifurcations permitted or required by the symmetries of the system should not eclipse the fact that it is the physics and geometry of the system that dictate its symmetries. Two features of the convective flows would seem to stand out as amenable to physical explanation. First, in the eigenmodes of the vertical layer, clockwise and counter-clockwise vortices are on an equal footing, as is dictated by symmetry (the eigenmodes must be trigonometric in z). However, in the finite-amplitude convective flows, both steady and traveling, the counter-clockwise vorticity has been banished to the sidewalls: Almost the entire layer is occupied by clockwise rotating vortices separated by stagnation points.

TABLE I. Critical $Ra_c(Le-1)$ of transcritical (TR) and of pitchfork (PF) bifurcations in closed cavities.

A	$Ra_c(Le-1)$ (TR)	$Ra_c(Le-1)$ (PF)	A	$Ra_c(Le-1)$ (TR)	$Ra_c(Le-1)$ (PF)
1.	17 163.87	25 898.28	2.15	8524.90	8493.46
1.1	14 411.83	21 501.78	2.3	8367.84	8123.13
1.2	12 624.77	18 296.75	2.5	8157.70	7781.91
1.3	11 421.62	15 899.85	2.65	7991.85	7607.28
1.4	10 588.50	14 073.65	2.8	7823.11	7482.14
1.5	9998.60	12 662.45	3.	7607.92	7369.61
1.6	9573.03	11 519.67	3.15	7463.17	7312.76
1.7	9260.50	10 690.03	3.3	7337.18	7270.40
1.8	9026.31	9999.07	3.5	7199.98	7224.86
1.9	8846.03	9446.75	3.65	7119.04	7191.94
2.	8701.83	9003.13	3.8	7054.85	7155.93
			4.	6991.37	7101.05

Second, in the square cavity, we have computed the branch of unstable steady states consisting of a clockwise rotating central cell bordered by small counter-rotating cells in opposite corners. This state will either decay to conduction or evolve to the finite-amplitude branch. In the latter case, the small counter-rotating corner cells will be excluded by the central cell, which will grow to occupy the entire cavity and will tilt in the opposite direction from the eigenmode. What physical mechanisms are responsible for destroying the counter-rotating corner cells and for reversing the tilt of the central cell? Why is the bifurcation so strongly transcritical; i.e., why does convection in the form of the single clockwise rotating cell of the finite amplitude branch subsist so far below the threshold for instability of the conductive state? Physical explanations undoubtedly exist for these basic phenomena.

We end by noting that the bifurcation diagrams are expected to become increasingly complicated as the aspect ratio is increased. Not only do the transcritical and pitchfork bifurcation thresholds approach one another, but there are also certainly many other bifurcating branches at only slightly larger Rayleigh numbers. The possible secondary and global bifurcations that may stabilize, destabilize, or connect these branches can lead to complicated transition scenarios that can only be predicted by detailed construction of the bifurcation diagrams. Ghorayeb and Mojtabi[5,6] have carried out simulations in rectangular cavities for aspect ratios ranging from $A=1$ to $A=7$, and have found multiple steady states, as many as four for $A=7$. Complete bifurcation diagrams for increasing values of A have yet to be constructed and analyzed.

[1] S. A. Thorpe, P. K. Hutt, and R. Soulsby, ''The effect of horizontal gradient on thermohaline convection,'' J. Fluid Mech. **38**, 375 (1969).
[2] R. Krishnan, ''A numerical study of the instability of double-diffusive convection in a square enclosure with horizontal temperature and concentration gradients, Heat transfer in convective flows'' (ASME Nat. Heat Transfer Conf., Philadelphia, 1989), p. 357.
[3] R. Bennacer, ''Convection naturelle thermosolutale: simulation numérique des transferts et des structures d'écoulement,'' Thèse de Doctorat, Univ. Paris VI, 1995.
[4] D. Gobin and R. Bennacer, ''Double diffusion in a vertical fluid layer: onset of the convective regime,'' Phys. Fluids **6**, 59 (1994).
[5] K. Ghorayeb and A. Mojtabi, ''Étude de la convection thermosolutale dans une cavité rectangulaire verticale fluide,'' C. R. Acad. Sci. Paris, Série II b **324**, 19 (1997).
[6] K. Ghorayeb and A. Mojtabi, ''Double diffusive convection in a vertical rectangular cavity,'' Phys. Fluids **9**, 2339 (1997).
[7] S. Xin, P. Le Quéré, and L. S. Tuckerman, ''Double diffusion in a square cavity: on the nature of the bifurcation at convection onset,'' Notes et Documents LIMSI, 96-07, 1996.
[8] U. Ehrenstein and R. Peyret, ''A Chebyshev collocation method for the Navier–Stokes equations with application to double-diffusive convection,'' Int. J. Numer. Methods Fluids **9**, 427 (1989).
[9] R. Peyret and J. M. Vanel, ''Numerical experiments in double-diffusive

convection,'' *Computational Fluid Dynamics*, edited by D. Lentloff and R. C. Srivastava (Springer, New York, 1995), p. 33.
[10]J. E. Hart, ''On sideways diffusive instability,'' J. Fluid Mech. **49**, 279 (1971).
[11]J. E. Hart, ''Finite amplitude sideways diffusive convection,'' J. Fluid Mech. **59**, 47 (1973).
[12]N. Tsitverbit and E. Kit, ''The multiplicity of steady flows in confined double-diffusive convection with lateral heating,'' Phys. Fluids A **5**, 1062 (1993).
[13]N. Tsitverbit, ''Bifurcation phenomena in confined thermosolutal convection with lateral heating: commencement of double-diffusive region,'' Phys. Fluids **7**, 718 (1995).
[14]J. S. Turner, ''Multicomponent convection,'' Annu. Rev. Fluid Mech. **17**, 11 (1985).
[15]C. Canuto, M. Y. Hussaini, A. Quarteroni, and T. A. Zang, *Spectral Methods in Fluid Dynamics* (Springer, New York, 1988).
[16]J. M. Vanel, R. Peyret, and P. Bontoux, *Numerical Methods for Fluid Dynamics II*, edited by K. W. Morton and M. J. Baines (Clarendon, Oxford, 1986), pp. 463–475.
[17]C. Bernardi and Y. Maday, *Approximations Spectrales de Problèmes aux Limites Elliptiques, Collection Mathématiques & Applications*, edited by J. M. Ghidaglia and P. Lascaux (Springer, New York, 1992).
[18]P. Le Quéré, Thèse d'Etat, Université de Poitiers, 1987.
[19]F. Abcha, Thèse de Doctorat, Université Paris VI, 1995.
[20]I. Goldhirsch, S. A. Orszag, and B. K. Maulik, ''An efficient method for computing leading eigenvalues and eigenvectors of large asymmetric matrices,'' J. Sci. Comput. **2**, 33 (1987).
[21]K. N. Christodoulou and L. E. Scriven, ''Finding leading modes of a viscous free surface flow: an asymmetric generalized eigenproblem,'' J. Sci. Comput. **3**, 355 (1988).
[22]C. K. Mamun and L. S. Tuckerman, ''Asymmetry and Hopf bifurcation in spherical Couette flow,'' Phys. Fluids **7**, 80 (1995).
[23]L. S. Tuckerman, ''Steady-state solving via Stokes preconditioning: Recurrence relations for elliptic operators,'' *Lecture notes in Physics*, edited by D. L. Dwoyer, M. Y. Hussaini, and R. G. Voigt (Springer, New York, 1989), p. 573.
[24]A. Bergeon, D. Henry, H. BenHadid, and L. S. Tuckerman, ''Marangoni convection in binary mixtures with Soret effect,'' J. Fluid Mech. (in press).
[25]J. D. Crawford and E. Knobloch, Annu. Rev. Fluid Mech. **23**, 341 (1991).
[26]P. Coullet, R. E. Goldstein, and G. H. Gunaratne, ''Parity-breaking transitions of modulated patterns in hydrodynamic systems,'' Phys. Rev. Lett. **63**, 1954 (1989).
[27]P. Coullet and G. Iooss, ''Instabilities of one-dimensional cellular patterns,'' Phys. Rev. Lett. **64**, 866 (1990).
[28]I. G. Kevrekidis, B. Nicolaenko, and J. C. Scovel, ''Back in the saddle again: A computer-assisted study of the Kuramoto-Sivashinsky equation,'' SIAM (Soc. Ind. Appl. Math.) J. Appl. Math. **50**, 760 (1990).
[29]S. Fauve, S. Douady, and O. Thual, ''Drift instabilities of cellular patterns,'' J. Phys. II **1**, 311 (1991).
[30]M. Kness, L. S. Tuckerman, and D. Barkley, ''Symmetry-breaking bifurcations in one-dimensional excitable media,'' Phys. Rev. A **46**, 5054 (1992).
[31]R. D. Henderson and D. Barkley, ''Secondary instability in the wake of a circular cylinder,'' Phys. Fluids **8**, 1683 (1996).